Research Article

Studying the Effects of Process Parameters on Bending Angle and Edge Effects in Laser Bending Process of Perforated Sheets

M. Safari* and J. Joudaki

Department of Mechanical Engineering, Arak University of Technology, Arak, Iran

ARTICLE INFO

ABSTRACT

Conventional bending processes for perforated sheets using steel dies often result in undesirable deformation of the holes along the bend line. In contrast, the laser bending process presents a suitable alternative for effectively bending these sheets. This study investigates the laser bending process of perforated sheets through experimental tests and numerical simulations, employing a finite element model for the simulations. The effects of process variables, including laser power, scanning speed, laser beam diameter, and the number of holes along the irradiating path, on the output parameters (bending angle and edge effects), are examined. The finite element simulation and experimental measurements demonstrate good agreement. Results indicate that the bending angle of laser-bent perforated sheets increases with higher laser power, larger laser beam diameter, reduced scanning speed, and fewer holes in the irradiation path. Furthermore, the lateral deformation of the free edges (edge effect) increases with greater laser power, reduced scanning speed, larger laser beam diameter, and higher number of holes in the irradiation path. The edge effect is influenced by the temperature gradient along the irradiation path; higher laser power generates elevated local temperatures and increased cooling rates, whereas higher scanning speed leads to a more uniform temperature distribution in the sheet.

© Shiraz University, Shiraz, Iran, 2024

1. Introduction

In recent years, the use of laser beams to bend sheets and tubes in various industries has rapidly expanded. Due to the unique features of this process, including its very high accuracy, absence of springback, and very few changes in the microstructure of the sheet, it has gained significant attention from researchers. Springback occurs in die press bending when the punch moves back during unloading. A tensile-compressive stress distribution occurs in the loading stage and the elastic strain is released by unloading and making minor changes in the bent angle (springback) [1]. The mechanism of laser bending, especially the temperature gradient mechanism (TGM), shows that the sheet bends

---

in the cooling stage (shrinkage). Therefore, no classical springback occurs, unlike in conventional press bending. The concentrated thermal load of the laser beam heats the sheet to a higher temperature which converts the BCC structure to an FCC structure. This higher temperature and the resulting microstructure evolution lead to the formation of a narrow heat-affected zone (HAZ) in the laser bending process. In this process, mechanical tools are not used to form the sheets, while the process of sheet forming is caused by the energy irradiated to the sheet and the absorbed energy in the form of thermal energy deforms the sheets and creates thermal strains, followed by plastic strains during the cooling stage. The main limitation of laser bending is the material type. Ceramics and polymer parts cannot be bent by the laser beam. The laser bending of bi-layer sheets has been conducted by the authors. Various studies have explored the laser bending of steel-titanium sheets [2], aluminum-copper two-layer sheets [3], steel-aluminum sheets [4], and functionally graded copper-aluminum sheets [5]. Additionally, higher thermal conductivity, higher light reflection and light transmission pose further limitations in this process. For example, the generated heat in copper sheets transfers rapidly and does not create a temperature gradient because of the high thermal conductivity of copper. The laser bending process can bend thick sheets more easily than thin ones due to the better formation of a temperature gradient. Recent years have seen various studies on the laser bending process (LBP), which we will review here.

Song et al. [6] studied the laser bending of high-strength steels through both experimental methods and finite element simulation. They found that increasing the absorption coefficient of laser-irradiated surfaces noticeably enhances the bending angle of the sheet. Maji et al. [7], in an experimental study, investigated the LBP of stainless steel sheets. They analyzed the effects of process variables, particularly the number of irradiation passes, using both mechanical and metallurgical observations. The bending angle was obtained by a regression equation derived from an analysis of variance. The optimum condition to maximize the bending angle

was determined. As a result of the laser bending, refined microstructure and higher microhardness were observed in the bent zone. Fetene et al. [8] compared the bending angle of a coated sheet with cement and a friction stir-processed sheet due to irradiation by the laser beam. The result shows that the absorption coefficient increased in both investigated sheets. In a similar study, Fetene et al. [9] investigated the changes in the bending angle by dimensions of the sheet in the laser bending of AH36 steel sheets. Multi-pass irradiations were performed experimentally and numerically. It was concluded that the bending angle increases by increasing the sheet width and reducing the strip thickness. Paramasivan et al. [10] studied the effect of forced cooling in LBP with numerical simulations. They concluded that the bending angle increases when using external forced cooling. Safari and Joudaki [11] utilized an artificial neural network for the prediction of bending angle in laser bending of tailored machined blanks (TMB). They concluded that accurate predictions could be achieved by neural networks in bending. LBP of two-layered steel-titanium sheets was studied by Kotobi et al. [2]. The residual stress distribution along the thickness during the bending of the sheet was investigated by numerical simulations. The results disclosed that tensile stresses increased by increasing the output power. Zhang et al. [12] investigated the edge effect phenomenon in the laser bending of dual-phase steel sheets. They found that the edge effect was reduced for the higher number of irradiation passes. Nath and Yadav [13] proposed an analytical model to calculate the temperature distribution and find the bending angle. The accuracy of the analytical model was compared with the finite element model and experimental results of AA 6061-T6 laser bending and found to be very good. The results show that the bending angle increases with increasing the sheet width. The edge effect increases with increasing sheet width and decreasing sheet length [14]. Seyedkashi et al. [15] studied the LBP of SUS304L/C11000 clad sheets. They studied the effects of scanning speed, laser power, and laser beam diameter on the bending angle of laser-bent cladded sheets. Li et al. [16] derived an analytical solution for the calculation of the bending angle of

laminated sheets in LBP. The equation is derived by predicting the temperature distribution and calculating the temperature gradient. The results show that the predicted bending angles from the suggested equation were in acceptable agreement with experimental results. Wang et al. [17] examined the thickening of laminated sheets in the LBP and concluded that along the irradiating path, the grain size was increased and this phenomenon leads to the thickening of the sheets.

The literature review shows that the LBP is an effective technique for bending sheets. The effect of the main process parameters was investigated by the researchers [18, 19]. To the authors' knowledge, there are only a limited number of publications addressing the laser bending of perforated sheets. A recent study was published that measured the bending angle by designing experiments based on the response surface methodology [20]. The perforated sheets are employed in different industries, including construction and architecture (e.g., signboards, ventilation grills, facades, temporary airfield surfaces, acoustic panels, site amenities, cladding, infill panels, sunshades, metal signage, fencing screens, and column covers), automotive (e.g., ventilation parts, grids, silencer tubes, radiator grills, boards, flooring, air and oil filters), and the chemical and energy sectors (e.g., purifiers, filters, washing equipment, drying baskets, battery separator plates), and material development (cinder screens, blast furnace screens, and cement slurry screens). These sheets are widely utilized for reducing the weight of structures and enhancing ventilation conditions.

As the use of perforated sheets increases, it is essential to investigate their behavior. Thus, the objective of this article is to explore the edge effect phenomenon and bending angle in the laser bending of perforated sheets through both experimental and numerical approaches. The bending of perforated sheets by conventional dies encounters several problems, mainly the ovality and deformation of the holes located at the centerline of the bend. LBP is a precise method for bending and this research attempted to bend perforated sheets using laser beam irradiation. In this way, the study examined the effects of process variables including the

laser power, scanning speed, laser beam diameter, and number of holes in the irradiating path on the output variable (bending angle and edge effects).

2. Experimental Tests

To perform experimental tests, a continuous carbon dioxide laser device was used. Tests were conducted using a Ressi laser beam machine (RT1310U). The machine has a maximum power output of 120 W. The experiments were carried out on mild steel sheets with sample dimensions of 75×50×1 mm. The surface of the samples is covered with graphite powder to enhance the laser beam absorption. Fig. 1 shows the experimental setup of LBP. In these experiments, the effects of laser output power (LOP), laser scanning speed (LSS), laser beam diameter (LBD), and the number of holes along the irradiating path (NOH) were investigated. The bending angle and the lateral displacement of the free edge of the sheet (referred to as the edge effect in this paper) were measured experimentally. The sheet was clamped along its width edge (50 mm). The vertical displacement of the free edge (referred to as Y-displacement) was also measured as defined in Fig. 1(b). The bending angle was calculated using trigonometric functions (tangent function). A MITUTOYO coordinate measuring machine (CRYSTA-Apex V544 model) was employed to measure the displacements of the free edges and to calculate the main and lateral bending angles. The edge effect, which is associated with the variation in bending angle along the free edge, is defined in this paper as the difference between the maximum and minimum vertical displacement values:
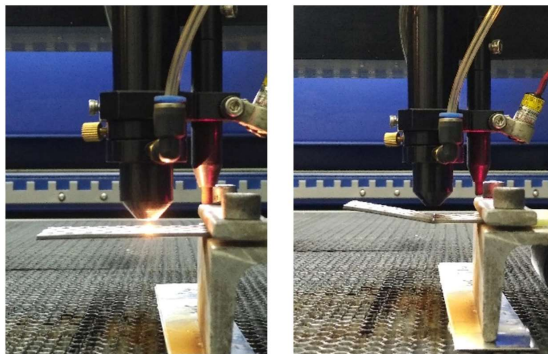
$$Edge\ effect = \frac{Y_{max} - Y_{min}}{Y_{max}} \times 100 \qquad (1)$$
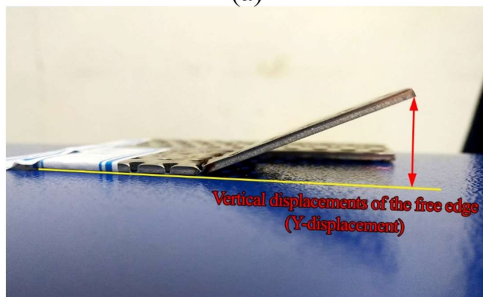
3. Numerical Simulation

The numerical simulation of the LBP of perforated sheets was conducted using the Abaqus/Implicit package. The LBP is a two-phase process, including both thermal and mechanical solutions, commonly referred to as thermomechanical simulation. This process means that, as a result of laser irradiation, the

irradiated areas experience thermal expansion and thermal contraction, which is followed by plastic deformation and, ultimately bending.

Abaqus, one of the most powerful software in simulating thermomechanical processes such as LBP, was used for the simulations in this study. It should be noted that in the LBP of perforated sheets, there are three important and critical areas during irradiation. The first area is the beginning of the hole, the second area is the end of the hole, and the third area is the area between the holes of the perforated sheet. The inner zone of the sheet experiences a higher temperature gradient, and therefore, the mesh in this area was refined. A mesh sensitivity analysis was conducted to select the mesh size. These three areas differ in terms of thermal and boundary conditions, which affect the final bending angle of perforated sheets. The dimensions of the perforated sheet were 75×50×1 mm, matching the experimental samples.

The mechanical and thermal properties of the perforated sheet are presented in Tables 1 and 2. In Abaqus, the laser bending simulations were performed using the Abaqus/standard solution. All degrees of freedom along one edge of the sheet (width) were fixed (Encastre). The LBP of perforated sheets was simulated in two steps: irradiation and cooling. During the irradiation step, heat flux was applied to the sheet along the irradiation line, defined by a DFLUX subroutine according to the process parameters. In the cooling step, the sheet was allowed to cool after laser irradiation. At this point, the sheet was permitted to reduce its temperature through heat transfer, returning to ambient temperature. The maximum temperature decrease per interval was limited to 50 °C to ensure temperature convergence.

The laser beam irradiation path is shown in Fig. 2(a). It can be seen that different areas of the sheet were meshed, and the laser beam path has a clear, regular, and uniform mesh, which aids in solving the problem accurately. The laser beam, irradiated along the line, passes through the center of the holes, maximizing the effect of the holes' presence. In the simulations, the employed element type is C3D8R, a 3D linear brick element with enabled reduced integration. Furthermore, the irradiation stage and the final displacement along the vertical direction after the cooling stage are depicted in Figs. 2(b) and 2(c).

(a)

Vertical displacements of the free edge (Y-displacement)
(b)

Fig. 1. (a) Bending of a perforated sheet during the laser bending process (LBP) and (b) definition of the vertical displacement of the free edge (Y-displacement).

Table 1. Thermal properties of the perforated sheets made of mild steel [21]

Temperature (°C)	Thermal conductivity (W/mm. °C)	Specific heat (kJ/kg. °C)
0	51.9×10^{-3}	486
100	51.1×10^{-3}	486
200	48.6×10^{-3}	498
300	44.4×10^{-3}	515
400	42.7×10^{-3}	536
500	39.4×10^{-3}	557
600	35.6×10^{-3}	586
700	31.8×10^{-3}	619
800	26.0×10^{-3}	691
900	26.4×10^{-3}	695
1000	27.2×10^{-3}	691

Table 2. Mechanical properties of the perforated sheets made of mild steel [21]

| Temperature (°C)	Elastic modulus (GPa)	Poisson's ratio	Coefficient of thermal expansion (1/°C)	Yield stress for $e_p = 0$ (MPa)	Yield stress for $e_p = 0.1$ (MPa)
20	206	0.296	0.117×10^{-4}	422.64	344.64
100	203	0.311	0.11×10^{-4}	409.93	331.93
200	201	0.330	0.122×10^{-4}	386.30	308.30
300	200	0.349	0.128×10^{-4}	342.57	276.07
400	165	0.367	0.133×10^{-4}	290.22	235.22
500	120	0.386	0.138×10^{-4}	230.77	185.77
600	60	0.405	0.144×10^{-4}	162.71	127.71
700	40	0.423	0.148×10^{-4}	96.05	68.55
800	30	0.442	0.148×10^{-4}	84.35	64.35
900	20	0.461	0.148×10^{-4}	60.65	46.65
1000	10	0.480	0.148×10^{-4}	21.32	11.32

(a)

(b)

(c)
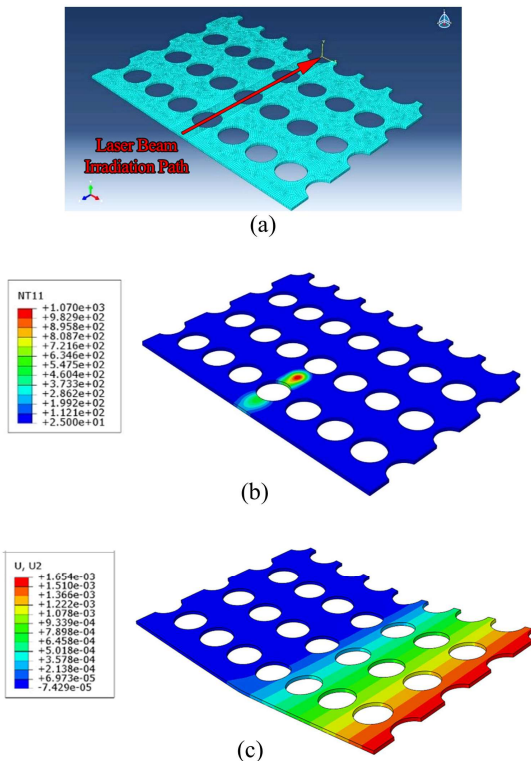
Fig. 2. (a) The mesh topology of the perforated sheet, (b) laser beam irradiation on the surface, and (c) vertical displacements of the free edge (Y-displacement) after the cooling stage.

4. Results and Discussion

After carrying out the finite element analysis and experimental measurements, the results of Y-displacement are prepared and analyzed to determine the effects of process parameters. Firstly, it is necessary to assess the validity of the finite element simulation. Fig. 3 shows a comparison between Y-displacements of the

perforated sheet obtained by experimental measurements and finite element results. As can be seen, the Y-displacement of points located on the free edge is not uniform as a result of laser irradiation, and there is a difference between the displacement of different points on this edge. This is caused by the difference in the heating conditions of different points as well as the boundary conditions of different points. In the references, the difference in the displacement of the points located on the free edge of the beam is known as the edge effect, and it is one of the most important issues of bending when using the laser beam for bending the sheets. Examining the data related to the Y-displacement for experimental measurements and numerical results shows that the edge effect (Eq. (1)) for experimental measurement and finite element simulation is 1.2% and 1.15%, respectively. It can be concluded that the numerical simulations are in good agreement with the experimental tests.
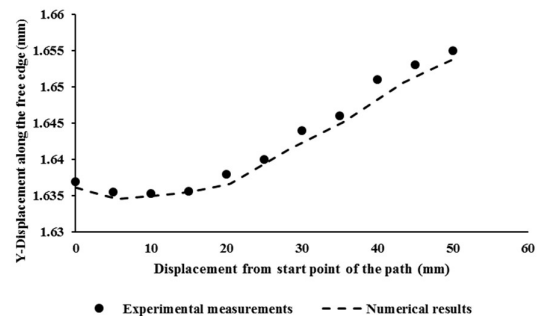

Fig. 3. Y-displacements of the points located on the free edge of the perforated sheet.

Fig. 4 shows the effect of laser output power (LOP) on the Y-displacement of the free edge. As mentioned, the Y-displacement varies along the free edge and the average value of Y-displacement is considered in plotting Fig. 4. The average value of Y-displacement of the free edge increases with an increase in the LOP. This is due to the transfer of higher heat fluxes irradiated onto the surface of the sheet, which creates higher thermal stresses and consequently higher plastic deformation in the cooling stage. Thus, a higher thermal gradient leads to higher vertical displacement of the free edge.

The effect of LOP on the edge effect is shown in Fig. 5. It can be concluded that as the LOP increases, the edge effects also increase. This is because the heat transfer rate depends on the input heat flux and the temperature of the sheet. With an increased heat transfer rate at higher laser power, more areas of the sheet are exposed to heat. However, the sheet is at ambient temperature at the start of the irradiation path while the temperature increases at the end of the irradiation path (due to heat transfer). Therefore, different areas with different boundary conditions and thermal conditions appear in the sheet. Thus, the edge effect increases with an increase in LOP.

Fig. 6 shows the effect of laser scanning speed (LSS) on the average value of Y-displacement of the free edge. The results show that the Y-displacement decreases as the LSS increases. This is due to the reduction of the heat flux irradiated to the surface of the sheet as the LSS increases. In other words, at a constant LOP, the total energy irradiated to the sheet decreases by increasing the LSS because of the shorter duration of laser irradiation on the sheet. Therefore, the plastic deformation areas are also reduced, and as a result, the average value of bending decreases. Fig. 7 shows the edge effect with respect to the LSS. As can be seen from this figure, the edge effect decreases as the LSS increases. The heat energy transferred to the sheet is reduced by increasing the scanning speed and then the areas experiencing the laser heating are also reduced in areas that have different boundary conditions and varying thermal conditions. As a result, the edge effects of the sheet are reduced. Fig. 8 shows the effect of LBD on the average value of Y-displacements of the free edge.
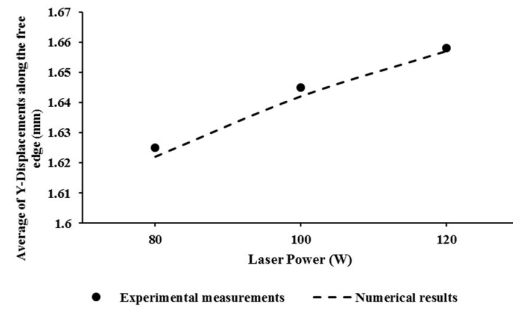

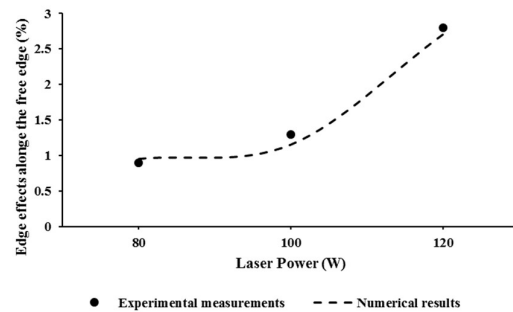**Fig. 4.** The effect of LOP on the average value of Y-displacements.

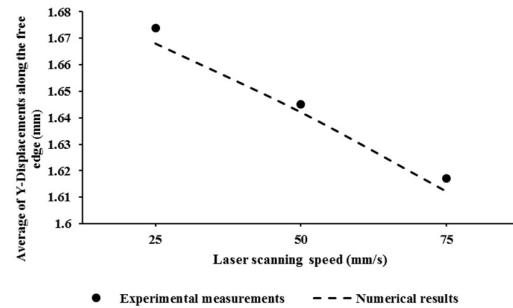**Fig. 5.** The effect of LOP on the edge effect of the free edge.

Fig. 6. The effect of LSS on the average value of Y-displacements.
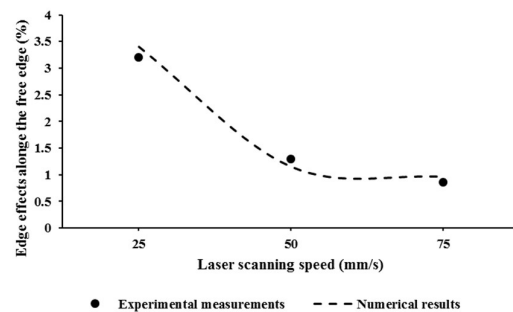

Fig. 7. The effect of LSS on the edge effect of the free edge.

By increasing the diameter of the laser beam, the average value of Y-displacements increases. This is because an increase in the diameter of the laser beam

results in the areas under laser irradiation, and therefore the plastic deformations also increase. As a result, the average value of Y-displacements of the free edge also increases.

Fig. 9 shows the variation of the edge effect in relation to the LBD. As can be seen, the edge effect exhibits a slight increase with an increase in LBD. This phenomenon could be attributed to the fact that, as the laser beam diameter increases, the irradiated areas also increase. This results in enhanced plastic deformations across regions with varying boundary conditions and thermal conditions, ultimately leading to an increase in the sheet's edge effect.

Fig. 10 shows the effect of the NOH on the average value of the Y-displacement of the sheet. The results show that the average value of Y-displacements decreases as the NOH increases. This can be attributed to the reduction in areas susceptible to plastic deformation due to laser irradiation as the NOH increases. The decrease in plastic deformation areas consequently leads to a reduction in the average value of Y-displacements.

Fig. 11 shows that the edge effect of the free edge increases with an increase in the NOH. This observation could be explained by the fact that, as the NOH increases, the stable regions of the sheet located between the holes effectively decrease. Therefore, as the volume of these regions with stable conditions decreases, the presence of regions with varying boundary and thermal conditions leads to an increase in the edge effects of the sheet.

5. Conclusion

The laser bending process (LBP) of perforated sheets was investigated experimentally and numerically. The effects of process variables such as laser output power (LOP), laser scanning speed (LSS), laser beam diameter (LBD), and number of holes (NOH) on the bending angle and also the edge effect of laser bent perforated sheet were examined.
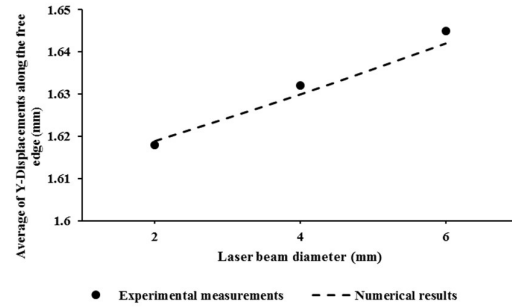

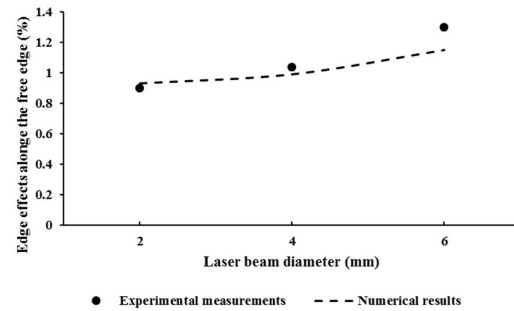**Fig. 8.** The effect of LBD on the average value of Y-displacements.

Fig. 9. The effect of LBD on the edge effect of the free edge.
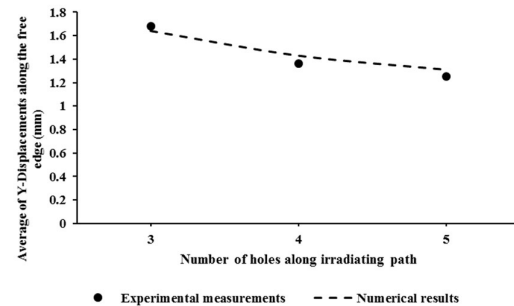

Fig. 10. The effect of the NOH on the average value of Y-displacements.
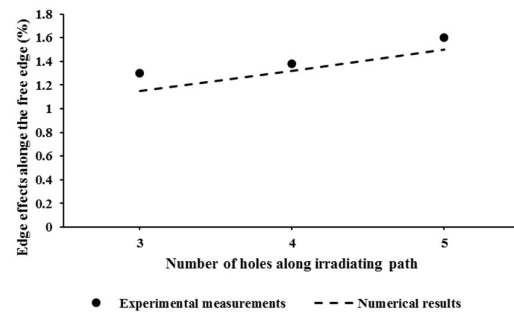

Fig. 11. The effect of the NOH on the edge effect of the free edge.

The main findings of this research can be listed as follows:

- A comparison between the experimental and numerical results demonstrated a good agreement between the finite element simulations and experimental findings.
- The results showed that the average value of Y-displacements increased with higher laser power. This is due to the increased heat transferred to the sheet as the laser output power (LOP) rises, resulting in larger areas of the sheet experiencing plastic deformation due to the applied heat. Additionally, the results indicated that as laser power increases, the edge effect also increases because of the varying heat transfer rates and temperatures within the sheet. Heat transfer raises the temperature along the scanning path, and variable temperature conditions coupled with different cooling rates contribute to the increase in the edge effect.
- The results led to the conclusion that the average value of Y-displacements decreased with increasing laser scanning speed (LSS). As the LSS increased, while keeping the LOP constant, the duration of laser irradiation was reduced, resulting in less energy being applied to the sheet. Consequently, the plastic deformation areas were also diminished. Moreover, the results revealed that the edge effects decreased due to the reduced heat input to the sheet, which in turn decreased the areas subjected to laser heating with varying boundary conditions.
- It was demonstrated that with increasing laser beam diameter (LBD), the average value of Y-displacements of the free edge increased. As the diameter of the laser beam expanded, the areas subjected to laser irradiation also increased, leading to greater plastic deformations. Furthermore, the edge effects of the free edge increased with an increase in LBD. This can be attributed to the fact that as the diameter of the laser beam increases, the areas under laser irradiation become larger, which in turn enhances the plastic deformation in regions with varying boundary conditions. The results showed that the average value of Y-displacement of the free

edge decreased with an increase in the number of holes (NOH). This occurred because the areas susceptible to plastic deformation due to laser irradiation were reduced as the NOH increased. In addition, the edge effect of the free edge of the laser-bent perforated sheet increased with a higher NOH. The remaining areas of the sheet (the areas located between the holes) effectively diminished as the NOH increased.

Conflict of interest

The authors also acknowledge no conflict of interest.

Authors' Contributions

Mehdi Safari: Conceptualization, methodology, validation, investigation, writing—original draft preparation, writing—review and editing supervision.

Jalal Joudaki: Formal analysis, data curation, visualization, writing—original draft preparation, writing—review and editing.

6. References

[1] Joudaki, J., & Sedighi, M. (2017). Effect of material's behavior on residual stress distribution in elastic–plastic beam bending: An analytical solution. *Proceedings of the Institution of Mechanical Engineers, Part L: Journal of Materials: Design and Applications, 231*(4), 361–372. https://doi.org/10.1177/1464420715597953

[2] Kotobi, M., & Honarpisheh, M. (2018). Through-depth residual stress measurement of laser bent steel–titanium bimetal sheets. *The Journal of Strain Analysis for Engineering Design, 53*(3), 130–140. https://doi.org/10.1177/0309324717753212

[3] Masoudi Nejad, R., Hoseini Shojaati, Z. S., Wheatley, G., & Ghahremani Moghadam, D. (2021). On the bending angle of aluminum-copper two-layer sheets in laser forming process. *Optics & Laser Technology, 142,* 107233. https://doi.org/10.1016/j.optlastec.2021.107233

[4] Ghoreishi, S. R., & Mahmoodi M. (2022). On the laser forming process of copper/aluminum bi-metal sheets with a functional thickness. *Optics & Laser Technology,* 149, 107870. https://doi.org/10.1016/j.optlastec.2022.107870

[5] Mazdak, S., Sheykholeslami, M. R., Gholami, M., Parvaz, H., Najafizadeh, M. M., Mahmoudi, S., & Vanaki, A. (2023). A statistical model for estimation of bending angle in laser bending of two-layer steel-aluminum sheets. *Optics & Laser Technology, 157*, 108575. https://doi.org/10.1016/j.optlastec.2022.108575

[6] Song, J. H., Lee, G. A., Jung, K. H., & Park, S. J. (2015). Laser irradiated bending characteristics of the ultra-high strength steel sheets. *International Journal of Automotive Technology, 16*, 89–96. https://doi.org/10.1007/s12239-015-0010-9

[7] Maji, K., Pratihar, D. K., & Nath, A. K. (2016). Experimental investigations, modeling, and optimization of multi-scan laser forming of AISI 304 stainless steel sheet. *The International Journal of Advanced Manufacturing Technology, 83*, 1441–1455. https://doi.org/10.1007/s00170-015-7675-0

[8] Fetene, B. N., Dixit, U. S., & Liao, H. (2017). Laser bending of friction stir processed and cement-coated sheets. *Materials and Manufacturing Processes, 32*(14), 1628–1634. https://doi.org/10.1080/10426914.2017.1279321

[9] Fetene, B. N., Kumar, V., Dixit, U. S., & Echempati, R. (2018). Numerical and experimental study on multi-pass laser bending of AH36 steel strips. *Optics & Laser Technology, 99*, 291–300. https://doi.org/10.1016/j.optlastec.2017.09.014

[10] Paramasivan, K., Das, S., Marimuthu, S., & Misra, D. (2018). Increment in laser bending angle by forced bottom cooling. *The International Journal of Advanced Manufacturing Technology, 94*, 2137–2147. https://doi.org/10.1007/s00170-017-1035-1

[11] Safari, M., & Joudaki, J. (2018). Prediction of bending angle for laser forming of tailor machined blanks by neural network. *Iranian Journal of Materials Forming, 5*(1), 47–57. https://doi.org/10.22099/IJMF.2018.28561.1097

[12] Zhang, Y., Dong, W., Qiao, Y., & Zhang, C. (2019). Edge effect investigation of DP980 steel sheet in multiple laser scanning process. *International Journal of Precision Engineering and Manufacturing, 20*, 319–326. https://doi.org/10.1007/s12541-019-00086-0

[13] Nath, U., & Yadav, V. (2022). Analytical modeling of temperature evolution and bend angle in laser forming of Al 6061-T6 sheets and its experimental analysis. *Optics & Laser Technology, 154*, 108307. https://doi.org/10.1016/j.optlastec.2022.108307

[14] Nath, U., Yadav, V., & Bhadauria, S. S. (2023). Effects of workpiece size on bending angle in laser forming of Al 6061-T6 sheet. *Materials Today: Proceedings.* https://doi.org/10.1016/j.matpr.2023.10.031

[15] Seyedkashi, S. M. H., Abazari, H. D., Gollo, M. H., Woo, Y. Y., & Moon, Y. H. (2019). Characterization of laser bending of SUS304L/C11000 clad sheets, *Journal of Mechanical Science and Technology, 33*, 3223–3230. https://doi.org/10.1007/s12206-019-0617-2

[16] Li, Z., & Wang, X. (2019). Analytical model for estimating bending angle in laser bending of 304 stainless steel/Q235 carbon steel laminated plate. *Journal of Laser Applications, 31*, 042012. https://doi.org/10.2351/1.5116729

[17] Wang, X., Ma, X., Li, Z., & Wang, R. A. (2016). Study of thickening phenomenon in laser bending zone of a metal laminated plate. *Procedia CIRP, 42*, 454–459. https://doi.org/10.1016/j.procir.2016.02.231

[18] Safari, M., de Sousa, R. A., & Joudaki, J. (2020). Recent advances in the laser forming process: a review. *Metals, 10*(11), 1472. https://doi.org/10.3390/met10111472

[19] Safari, M. (2020). A Study on the laser tube bending process: effects of the irradiating length and the number of irradiating passes. *Iranian Journal of Materials Forming, 7*(1), 46–53. https://doi.org/10.22099/ijmf.2019.34213.1133

[20] Safari, M., Babaei, A. M., Zamzami, B., & de Sousa, R. A. (2024). Experimental investigation, statistical modeling and optimization of laser bending process of perforated sheets. *Optics & Laser Technology, 175*, 110810. https://doi.org/10.1016/j.optlastec.2024.110810

[21] Safari, M., Farzin, M., Ghaei, A. (2013). Investigation into the effects of process parameters on bending angle in the laser bending of tailor machined blanks based on a statistical analysis. *Journal of Laser Applications, 25*(5), 052001. https://doi.org/10.2351/1.4811839